INTERNATIONAL JOURNAL OF PRECISION ENGINEERING AND MANUFACTURING Vol. 18, No. 10, pp. 1463-1473 OCTOBER 2017 / 1463

REGULAR PAPER

DOI: 10.1007/s12541-017-0174-5
ISSN 2234-7593 (Print) / 2005-4602 (Online)

Designing a Horizontal-Axis Wind Turbine for South Khorasan Province: A Case Study

Mehdi Jahangiri[1] and Akbar Alidadi Shamsabadi[2,#]

1 Department of Mechanical Engineering, Faculty of Technical Engineering, Shahrekord Branch, Islamic Azad University, Shahrekord, 88137-33395, Iran
2 Young Researchers and Elite Club, Shahrekord Branch, Islamic Azad University, Shahrekord, Iran
Corresponding Author / E-mail: a.alidadi@srbiau.ac.ir, TEL: +98-3833361099, FAX: +98-3833361099

KEYWORDS: Wind energy, Horizontal-axis wind turbine (HAWT), Weibull distribution, Fadashk station

Climate change, population and economic growth, increasing fossil fuel prices and environmental issues together emphasize the generation of electricity through wind. The potential of wind for generating clean energy is remarkable in many parts of Iran. In this study, a statistical analysis was performed on wind data of Fadashk Station located in South Khorasan province in north east of Iran. Accordingly, a horizontal-axis wind turbine (HAWT) was designed for this station. Wind speed was studied in deferent months of the year at 10 m, 30 m and 40 m heights. In the mentioned heights, this station had a mean speed of 5.27, 6.20, and 6.33 m/s, respectively. Direction of the prevailing wind is almost fixed throughout the year and blows from southeast. Power density was obtained by estimating the potential of wind energy using Weibull probability distribution function. Furthermore, the amount of energy that could be obtained annually from this site was calculated by selecting two wind turbines, Kuriant18 turbine made by Kuriant Company and Vestas55 made by Vestas Company, in the actual state. Also, annual mean wind power density in this station was estimated 285 W/m^2.

Manuscript received: January 17, 2017 / Revised: June 8, 2017 / Accepted: June 10, 2017

NOMENCLATURE

A = Rotor swept area (m²)
c = Weibull scale factor
c_i = Chord length, (m)
C_l = Two-dimensional lift coefficient
C_d = Two-dimensional drag coefficient
C_P = Power coefficient
$\overline{E}$ /A = Wind energy density (W/m^2)
E_w = Wind machine energy (Wh)
F = Tip loss correction factor
k = Weibull shape factor
N = Number of long-term data points
p(U) = Probability density function (PDF)
P_w(U) = Power curve of the wind turbine
$\overline{P}$ /A = Average wind power density
$\overline{P}_w$ = Average wind machine power
TI = Turbulence intensity
U = Wind speed (m/s)
$\bar{U}$ = Mean wind speed (m/s)
α = Angle of attack
α_i = Axial contraction
α_i' = Angular contraction
θ_P = Section pitch angle
θ_T = Blade twist angle
ρ = Air density (1.225 kg/m^3)
η = Drive train efficiency
φ_i = Relative velocity angle
λ = Tip speed ratio
$\Gamma(x)$ = Gamma function
σ = Solidity
σ_u = Standard deviation of wind speed
σ' = Local rotor solidity

1. Introduction

Energy has a direct influence on every human activity and plays an important role in human welfare and social and economic development

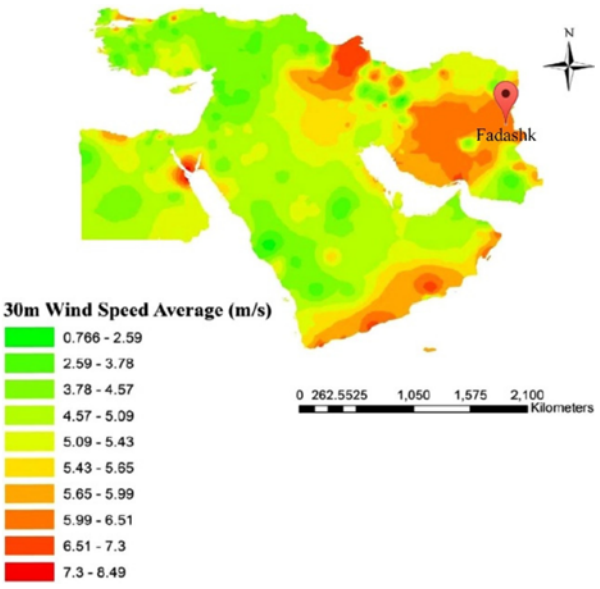

Fig. 1 Average wind speed in Middle-East and parts of Africa and Europe at a height of 30 m[30] (Fadashk is marked with map marker)

as it is undoubtedly an essential component of the modern life and society.[1-3] However, given the increasing global demand for energy, concerns about energy security such as fossil fuels availability and our dependence on them, greenhouse gas emissions and environmental degradation caused by energy produced from fossil fuels, and discussions regarding the effectiveness of the future of fossil fuels are considered crucial issues.[4-6] Population growth and industrial advances in many developing countries have led to the continuous increase in energy consumption. According to the International Energy Agency (IEA) the global energy consumption will increase by 37% to 2040.[7] In Iran, during the period between 1967-2007, consumption of ultimate fossil fuels increased around 617% and CO_2 gas emission was also increased about 610%.[8] This amount is also increasing day by day and this is a major challenge for policy makers and the society. Although fossil fuels will be the most important energy source in the world until 2030, various countries increasingly prefer to move towards a new energy source called renewable energies.[9] Renewable energy sources are appropriate replacement for fossil fuels and are basically considered as a sustainable, free, accessible, and clean source.[10-12] Using renewable energies has basically become as a strategic selection in the world for solving environment pollution, energy crisis, and achieving sustainable social development.[13] Moreover, initial surveys of public opinion showed high levels of support for utilizing renewable energies, particularly for the power of wind energy.[14] Wind energy is one of the most important sources of renewable energy for its benefits such as being clean, indigenous, inexhaustible and eco-friendly[15,16] and attractive in economic terms.[17] This energy, with an average growth rate of 30%, has been one of the fastest growing renewable energy sources over the world during the last decades.[18] Using wind energy could be an important parameter in people's daily lives in developing countries, where almost one third of the world's people live without electricity.[19,20] The history of wind turbines originates around 200 B.C

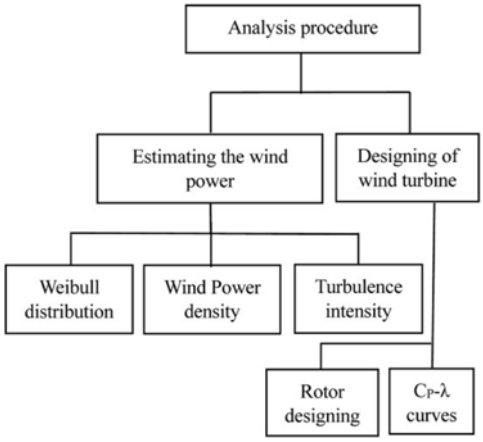

Fig. 2 Overview of the structure of the paper

somewhere in Persia but the first practical wind mills were developed in Iran in 7th century and were called Sistan wind mills.[21] Manjil and Roodbar were the first areas in which wind turbines were installed dates back to 1994. At first, two sets of 500 kW Nordtank wind turbines were installed. They produced more than 1.8 million kWh per year.[22] Of course many studies were performed regarding the potential level of wind energy in different parts of Iran. For example, in the city of Shahrbabak in Kerman province,[23] Mah-shahr station in Khuzestan province,[19] Tabriz and Ardabil,[24] Tehran,[25] Bushehr,[26] Yazd,[27] Zahedan[28] and Binalood in Razavi Khorasan province.[29] Fadashk station is located 44 kilometers from Birjand, the provincial capital of South Khorasan and its latitude and longitude are 32°78′ and 58°79′ respectively. In this paper, the potential of wind energy in Fadashk station was studied in 12 consecutive months of the year. In a period of one year, from 1/1/2007 to 12/31/2007, wind speed and wind direction data were used for the mentioned site in the time interval of 10 min. Fig. 1 shows the average wind speed in Middle-East and parts of Africa and Europe at a height of 30 m and indicates that eastern, central and south western parts of Iran. Wind energy potential in this station was calculated using Weibull distribution function. In addition, power generation potential by two wind turbines, whose performance diagrams are available for different speeds, was calculated.

2. Analysis Procedure

The Overview of the structure of this paper is shown in Fig. 2.

2.1 Weibull distribution

Statistical methods are used for determining the wind energy potential at a specific site and estimating its energy output. Frequency distribution of wind speed was presented using different probability density functions such as: Weibull Rayleigh, three parameter beta, lognormal, and gamma distributions. Weibull distribution is one of the common methods for determining wind energy potential.[31] If time series measured data are available at the desired location and height, there may be little need for a data analysis in terms of probability distributions and statistical techniques. On the other hand, if projection

of measured data from one location to another is required, or when only summary data are available, then there are distinct advantages to the use of analytical representations for the probability distribution of wind speed.[32] The probability density function may be used to express the probability of a wind speed occurring between U_a and U_b.[32]

$$p(U_a \le U \le U_b) = \int_{U_a}^{U_b} p(U)dU \tag{1}$$

Also, the total area under the probability density curve is given by:

$$\int_c^{\infty} p(U)dU = 1$$

One of these functions that has been validated by measuring in different parts of the world is Weibull probability density function that requires two parameters of k, a shape factor, and c, a scale factor. Both of these parameters are functions of $\bar{U}$ and σ'.[32]

$$p(U) = \left(\frac{k}{c}\right)\left(\frac{U}{c}\right)^{k-1} \exp\left[-\left(\frac{U}{c}\right)^{k}\right] \tag{2}$$

The cumulative density function (CDF) is expressed as:

$$F(U) = 1 - \exp\left[-\left(\frac{U}{c}\right)^{k}\right] \tag{3}$$

The following empirical relations were used to determine c and k:[32]

1. The empirical relation proposed by Justus

With standard deviation and mean wind speed, c and k factors could be achieved using the following formula.

$$k = \left(\frac{\sigma_U}{\overline{U}}\right)^{-1.086} \tag{4}$$

$$c = \frac{\overline{U}}{\Gamma\left(1+\frac{1}{k}\right)} \tag{5}$$

The gamma function, $\Gamma(x)$, is also calculated as follows:[23]

$$\Gamma(x) = \int_0^{\infty} e^{-u} u^{x-1} du$$

2. Lysen's empirical relation

In the above method, "k" factor was obtained from Eq. (4) at first and then the amount of "c" was obtained using the following equation.[32]

$$\frac{c}{\overline{U}} = \left(0.568 + \frac{0.433}{k}\right)^{-\frac{1}{k}} \tag{6}$$

2.2 Wind power density

Wind power density (W/m²) depends on air density (ρ) at the sea level and with a mean temperature of 15ºC and a pressure of 1 atm and the cube of the wind speed. The average wind power density was defined as follows:[32]

$$\frac{\overline{P}}{A} = \frac{1}{2}\rho\frac{1}{N}\sum_{i=1}^{N} U_i^3 \tag{7}$$

Also the wind energy density per unit area in a given time interval is:[32]

$$\frac{\overline{E}}{A} = \frac{1}{2}\rho\Delta t\sum_{i=1}^{N} U_i^3 = \left(\frac{\overline{P}}{A}\right)(N\Delta t) \tag{8}$$

The average wind machine power ($\overline{P}_w$), is:[32]

$$\overline{P}_w = \frac{1}{N}\sum_{i=1}^{N} P_w(U_i) \tag{9}$$

$\overline{P}_w(U_i)$ is the power output defined by a wind machine power curve and the energy from a wind machine (E_w), is: [32]

$$E_w = \sum_{i=1}^{N} P_w(U_i)(\Delta t) \tag{10}$$

2.3 Turbulence intensity

Wind turbulence occurs due to loss of the wind's kinetic energy and its conversion to thermal energy because of formation and destruction of small vortices. In a long period, wind turbulence maybe fixed but it is highly variable in small time intervals. Flow turbulence usually occurs due to surface roughness (of trees, building, etc.) and high altitude of the surface. Furthermore, the existence of turbulence in wind flow not only reduces its power, but also leads to the fatigue phenomenon in the wind turbine.[33] One of the measurement criteria of turbulence is turbulence intensity that is defined by the standard deviation of the wind speed divided by mean wind speed:[32]

$$TI = \frac{\sigma_U}{U} \tag{11}$$

Turbulence intensity is frequently in the range of 0.1 to 0.4. [32] In which standard deviation and mean velocity are usually calculated in the time interval of 10 min.

2.4 Rotor designing

Rotor design method begun with selecting different parameters of the rotor and was continued with selecting an appropriate airfoil type. An initial and appropriate form of the blade was determined by considering the rotary vortex. The final form and performance of the blade could be optimized using the iterative method and considering the drag, edge losses and construction parameters. Finally, the following steps could be considered for designing the blade.

2.4.1 Determining parameters of the rotor base

Given the desired power and mean wind speed in that location, by selecting C_p and η, radius of the blade was obtained using the following equation.[32]

$$p = C_p\eta \times \frac{1}{2} \times \rho\pi R^2 U^3 \tag{12}$$

"η" (Drive train efficiency) is part of the specifications of each turbine that with determining the type of turbine, Its value is determined. Also, C_p Obtained from the C_p-λ curve each turbine and by determining "λ". According to the type of application, choose a tip speed ratio, λ. For instance, for a water-pumping windmill that need bigger torque, use $1 < \lambda < 3$ and for electrical power generation, the proper selection is $4 < \lambda < 10$.[32] The appropriate number of blades could be selected according to Table 1. If blades number is less than 3, dynamic problems of the

Table 1 Suggested blade number, B, for different tip speed ratios, λ[32]

λ	1	2	3	4	>4
B	8-24	6-12	3-6	3-4	1-3

structure should also be taken into consideration for designing the hub.

Proper airfoil was selected according to the λ. If $\lambda < 3$, curved plates can be used. If $\lambda > 3$ use a more aerodynamic shape. Considering the selected airfoil type in the previous step, the next step is the choice of the design aerodynamic conditions, $C_{l,design}$ and α_{design}, such that $C_{d,design}/C_{l,design}$ is at a minimum for each blade section (Considering Figs. 11 and 12). The blade is divided into N elements (usually 10-20). The form of the "ith" section of the blade with a radius of r' was estimated using the optimized rotor theory. By combining the empirical results of previous steps and using the following equations, pitch (θ_P) and twist (θ_T) angles for each part of the airfoil could be obtained using the iterative method.

$$\lambda_{r,i} = \lambda\left(\frac{r_i}{R}\right) \tag{13}$$

$$\varphi_i = \left(\frac{2}{3}\right)\tan^{-1}\left(\frac{1}{\lambda_{r,i}}\right) \tag{14}$$

Afterwards, θ_P and θ_T angles were obtained using the following equations.

$$c_i = \frac{8\pi r_i}{BC_{i,design}}(1-\cos\varphi_i) \tag{15}$$

$$\varphi_i = \theta_{p,i} + \alpha_{design} \tag{16}$$

$$\theta_{T,i} = \theta_{p,i} - \theta_{p,o} \tag{17}$$

For convenience in making the blade, linear changes of the chord's length, thickness and twist were considered. In order to achieve this objective, variation function of the chord's length and twist distribution were expressed using the following functions.

$$c_i = a_1 r_i + b_1 \tag{18}$$

a_1, b_1 and a_2 coefficients could be obtained using curve fitting. The following two methods could be used for optimizing the initial dimensions of the blade:

1. Iterative method for obtaining α and C_l

By dividing the blade into N elements with equal lengths, the airfoil n with different angles of attack and consequently different lift and drag coefficients was obtained. The above method lies on the fact that based on the twist angle variations in the airfoil's length (from the hub up to the tip), angle of attack in each section of the airfoil will change. Find the actual angle of attack and lift coefficients for the center of each element, using the following equations and the empirical airfoil curves:[32]

$$\varphi_{i,1} = \left(\frac{2}{3}\right)\tan^{-1}\left(\frac{1}{\lambda_{r,i}}\right) \tag{19}$$

Loss coefficient in the blade's tip and the solidity of the blade was calculated through the following formulas. The correction factor (F) is a function of the number of blades, the angle of relative wind, and the position on the blade.[32]

$$c_{l,i} = 4F_i \sin\varphi_i \frac{(\cos\varphi_i - \lambda_{r,i}\sin\varphi_i)}{\sigma_i(\sin\varphi_i + \lambda_{r,i}\cos\varphi_i)} \tag{20}$$

Local rotor solidity can be calculated from:

$$\sigma' = \frac{Bc}{2\pi r_i} \tag{21}$$

$$F_i = \left(\frac{2}{\pi}\right)\cos^{-1}\left[\exp\left[-\left\{\frac{\left(\frac{B}{2}\right)\left[1-\left(\frac{r_i}{R}\right)\right]}{\left(\frac{r_i}{R}\right)\sin\varphi_i}\right\}\right]\right] \tag{22}$$

By changing the angle of attack, the amount of the φ' also changed and the calculations continued until the C_l resulted from Eq. (22) was equal to the C_l resulted from the first step (empirical results of the airfoil).

$$\varphi_{i,j+1} = \theta_{p,i} + \alpha_{i,j} \tag{23}$$

2. Iterative solution for obtaining a and a' coefficients

This method is based on iteration and an attempt is made to obtain the a amount of axial contraction coefficient and a' angle. Initial estimation of these amounts was obtained from the following equations derived from optimum blade design theory.

$$a_{i,1} = \frac{1}{\left[1+\frac{4\sin^2(\varphi_{i,1})}{\sigma'_{i,design}C_{i,design}\cos\varphi_{i,1}}\right]} \tag{24}$$

$$d_{i,1} = \frac{1-3a_{i,1}}{(4a_{i,1})-1} \tag{25}$$

With having $a_{i,1}$ and $a'_{i,1}$ coefficients, start the iterative solution procedure for the jth iteration. For the first iteration $j = 1$. Calculate the angle of the relative wind and the tip loss factor:[32]

$$\tan\varphi_{i,j} = \frac{U(1-a_{i,j})}{\Omega r(1+a'_{i,j})} = \frac{1-a_{i,j}}{(1+a'_{i,j})\lambda_{r,i}} \tag{26}$$

$$F_{i,j} = \left(\frac{2}{\pi}\right)\cos^{-1}\left[\exp\left[-\left\{\frac{\left(\frac{B}{2}\right)\left[1-\left(\frac{r_i}{R}\right)\right]}{\left(\frac{r_i}{R}\right)\sin\varphi_{i,j}}\right\}\right]\right] \tag{27}$$

Then, determine $C_{l,i,j}$ and $C_{d,i,j}$ from the airfoil lift and drag data, using:

$$\alpha_{i,j} = \varphi_{i,j} - \theta_{p,i} \tag{28}$$

Calculate the local thrust coefficient:

$$C_{T_r,i,j} = \sigma'_i(1-a_{i,j})^2 \times \frac{(C_{l,i,j}\cos\varphi_{i,j} + c_{d,i,j}\sin\varphi_{i,j})}{\sin^2\varphi_{i,j}} \tag{29}$$

If $C_{T,i,j} < 0.96$, a and a' coefficients could be obtained using the following equation.

$$a_{i,j+1} = \frac{1}{\left[1+\frac{4F_{i,j}\sin^2(\varphi_{i,j})}{\sigma'_i C_{I,i,j}\cos\varphi_{i,j}}\right]} \tag{30}$$

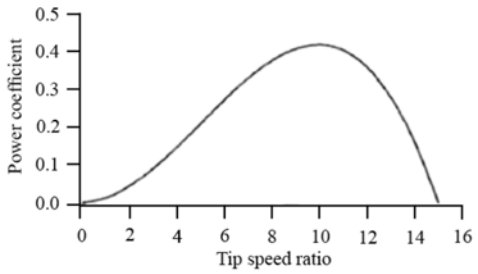

Fig. 3 Sample C_P-λ curve for a high tip speed ratio wind turbine[32]

If $C_{T,ij} > 0.96$, a and a' coefficients could be obtained using the following equation.

$$a_{i,j} = \left(\frac{1}{F_{i,j}}\right) \times [0.143 + \sqrt{0.0203 - 0.6427(0.889 - C_{T,i,j})}] \quad (31)$$

$$a'_{i,j+1} = \frac{1}{\frac{4F_{i,j}\cos\varphi_{i,j}}{\sigma' C_{l,i,j}}} \quad (32)$$

If the newest induction factors are within an acceptable tolerance of the previous guesses, then the other performance parameters can be calculated. If not, then the procedure starts again at Eq. (26) with $j = j+1$.[32] After completing the previous step and determining blade performances, the power coefficient could be obtained using the following equation.[32]

$$C_p = \frac{8}{\lambda N}\sum_{i=k}^{N} F_i \sin^2\varphi_i(\cos\varphi_i - \lambda_{ri}\sin\varphi_i) \times (\sin\varphi_i + \lambda_{ri}\cos\varphi_i) \times \left[1 - \left(\frac{Cd}{Ci}\right)\cot\varphi_i\right]\lambda_{ri}^2 \quad (33)$$

According to Eq. (33), the total length of the hub and blade is assumed to be divided into N equal length blade elements. Where k is the index of the first 'blade' section consisting of the actual blade airfoil.[32]

2.5 C_P-λ curves

By determining the optimum design of blade in λ_{design}, blade's performance in other amounts of λ should also be specified. This could be achieved using the method described in the previous section. C_P-λ curve allows us to predict the blade's behavior in different combinations of wind speed and rotor. Also, this curve gives us interesting information regarding C_P and $\lambda_{optimum}$. An example of C_P-λ curve has been presented in Fig. 3.

3. Results and Discussion

Two probability distributions are commonly used in wind data analysis: (1) the Rayleigh and (2) the Weibull. The Rayleigh distribution uses one parameter: the mean wind speed. The Weibull distribution is based on two parameters and, thus, can better represent a wider variety of wind regimes. The dataset is used to determine the wind characteristics of the region by using the Weibull distribution function. The Fadashk region in the south Khorasan is adopted for designing this site specific wind turbine.

Table 2 Calculation of parameters related to wind speed and power

Fadashk station			
Height (m)	40	30	10
Mean speed (m/s)	6.33	6.20	5.27
Wind power (W)	285.15	268.43	173.98
Energy factor	1.99	2.00	2.186

Table 3 Windiness assessment at the Fadashk station

Fadashk station				
Assessment type	Poor	Marginal	Good	Excellent
Number of months	2	4	1	5

Fig. 4 Monthly mean speed distribution in the Fadashk station

Numbers of analyzed wind speed data were 52559 in the time interval of 10 min. Wind speed data collected over a period of one year (from 1/1/2007 to 12/31/2007) at 10 m, 30 m and 40 m heights. The meteorological masts with 40 m height were installed in suitable coordinates by power ministry. The data logger used has 3 sensors of velocity at 10 m, 30 m and 40m heights and also 2 sensors of direction at 30m and 37.5 m. Parameters of wind speed and power resulted from the statistical analysis of the mentioned three heights are presented in Table 2.

As it can be seen, having an annual mean speed of $\bar{U}$ = 6.33 m/s, Fadashk station is capable of generating maximum power of P = 285.15 W. Monthly mean speed distribution is presented in Fig. 4. For the Fadashk station, maximum speed was in March with maximum monthly mean speed of $\bar{U}$ = 9.7 m/s, and minimum speed was in September with minimum monthly mean speed of $\bar{U}$ = 2.81 m/s. Since the potential value for annual mean wind speed at 10 m height is assessed as poor for mean speed lower than 4.5 m/s, marginal for 4.5-5.4 m/s, and good to very good for 5.4-6.7 m/s, and is excellent for speeds higher than 6.7 m/s[27]; therefore, Fadashk station could be categorized according to Table 3 in terms of windiness assessment.

Fig. 5 presents the monthly variations of the wind power density in heights of 10, 30 and 40 m above the ground level. As it is evident, maximum power was in March P = 720 W and minimum power occurred in September P = 45 W.

Wind rose is a diagram that shows the temporal distribution of wind direction and azimuthal distribution of wind speed at a given location. In Fig. 6, wind rose diagram is presented based on time (frequency) of

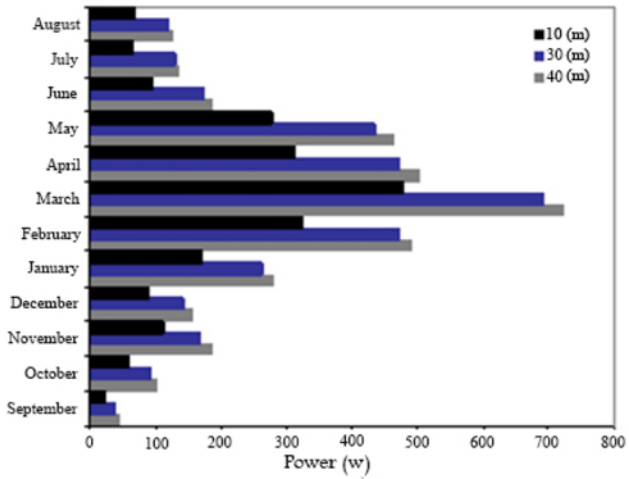

Fig. 5 Monthly mean power variations in the Fadashk station

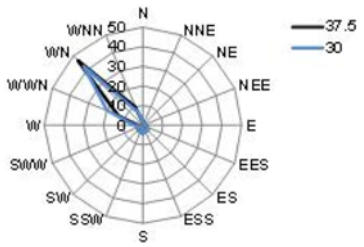

Fig. 6 Wind rose diagram based on wind blow frequency in 37.5 and 30 m heights

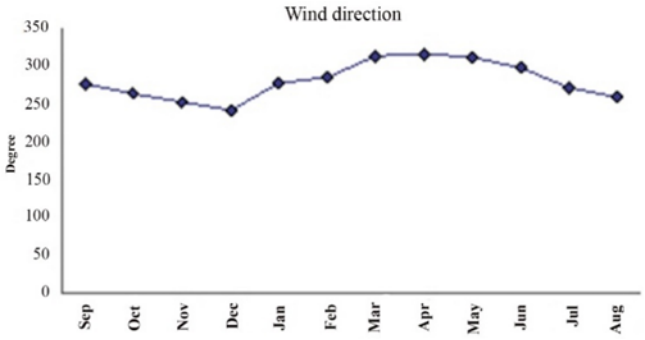

Fig. 7 Distribution of the prevailing wind direction throughout the year in the Fadashk station

wind blowing in 37.5 and 30 m heights. According to the Fig. 6, it could be claimed that all winds blew towards northwest or near that direction.

Fig. 7 shows the prevailing wind direction throughout the year for the Fadashk region. Wind direction was almost fixed throughout the year and blew from southeast. These issues are important for arranging turbines and the fixed wind direction is a major advantage for wind power plants.

Weibull distribution function was drawn using Matlab software. In order to compare and validate the presented equations for calculating shape and scale factors (Eqs. 4, 5 and 6), in Table 4 these coefficients

Table 4 Comparing different methods for achieving coefficients used in Weibull function

Eq. (6)		Eq. (5)		Matlab software		Station
Scale factor	Shape factor	Scale factor	Shape factor	Scale factor	Shape factor	
5.45	1.88	6.94	1.88	7.18	1.87	Fadashk

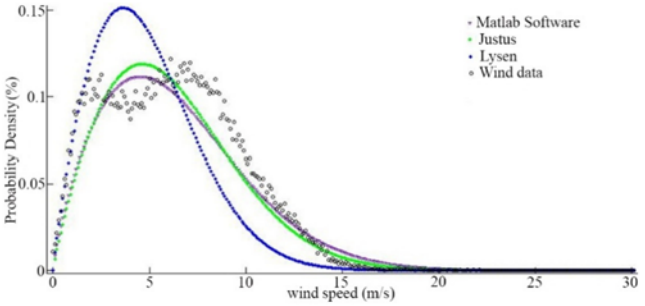

Fig. 8 Weibull distribution function

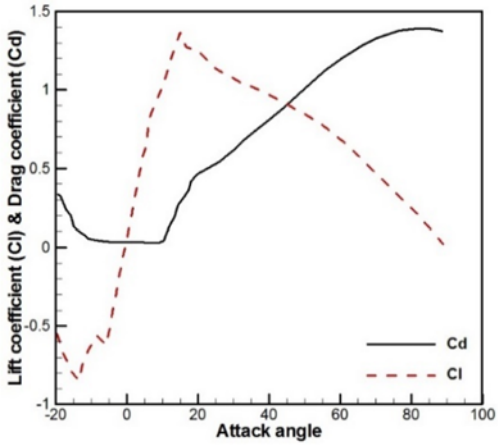

Fig. 9 Lift and drag coefficients, C_l and C_d, respectively, for the S809 airfoil

were calculated and collected using Matlab software and through the proposed equations.

It can be seen that Lysen's empirical equation has less accuracy than Justus' equation. Accuracies of these methods are shown in Fig. 8. As it can be seen in Fig. 8, Weibull's curve had good compatibility with measured speeds. Selecting an appropriate λ is the first parameter that should be considered in the blade's designing process.[34] In many modern turbines, λ coefficient is between the $6 \leq \lambda \leq 8$ ranges but proper selection of λ coefficient varies from one airfoil to another depending on the required power.

S809 airfoil[35] was used in this project. Fig. 9 shows the lift and drag coefficients curve based on angle of attack for the S809 airfoil. Digitizer software was used for fitting lift and drag curves. In order to have accurate calculations, 101 points where used for fitting each one of the curves.

This software's output could be imported by Matlab software. C_l and C_d curves were fitted using the "Curve Fitting Tool" in the Matlab

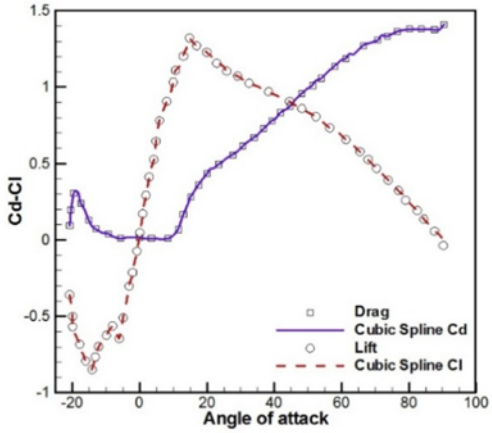

Fig. 10 Curve fitting using Matlab software (Between each 4 points, a third-degree curve to be drawn)

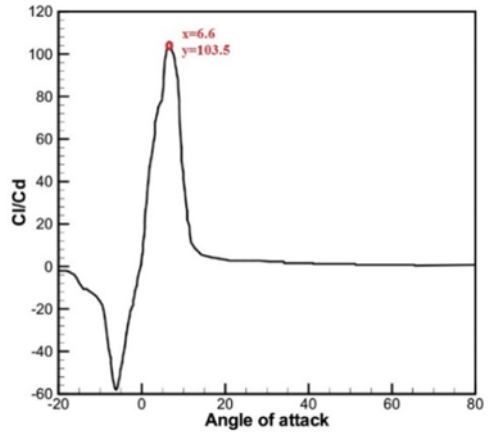

Fig. 11 C_l/C_d versus the angle of attack (the most efficient angle of attack is shown by a circle)

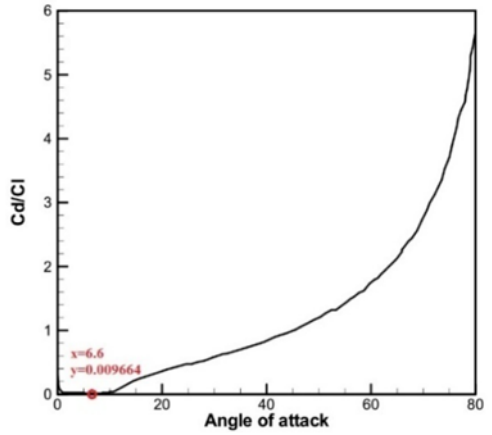

Fig. 12 C_d/C_l versus the angle of attack (the most efficient angle of attack is shown by a circle)

software. Fig. 10 shows how to perform fitting using the Matlab software.

In order to obtain α_{design}, $C_{l,design}$, and $C_{d,design}$, C_l/C_d and C_d/C_l diagram

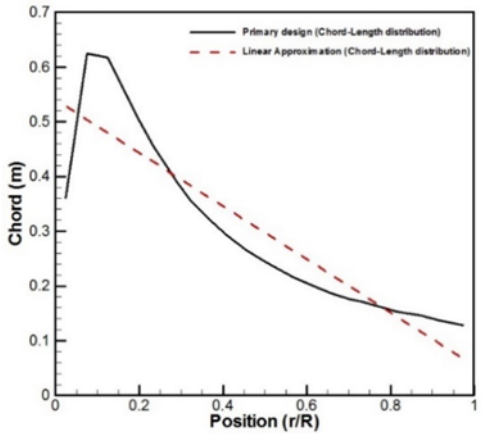

Fig. 13 Chord-length distribution versus position

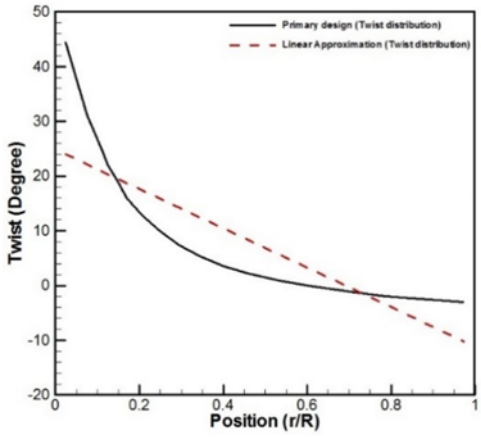

Fig. 14 Twist distribution in the initial design

were draw in Figs. 11 and 12 respectively.

As it can be seen, the optimal angle of attack was α_{design} = 6.6 and optimal lift and drag coefficients were respectively $C_{l,design}$ = 0.8229 and $C_{d,design}$ = 0.008 considering Fig. 9. Length of the chord line was divided into 20 equal elements and C_P-λ = 7 was selected for initial calculations. On the other hand, numbers of blades were selected, B = 3 according to Table 1. Initial calculations were performed for determining C_i, $\theta_{P,i}$, and $\theta_{T,i}$ coefficients. Initial results are presented in Figs. 13 and 14.

The considered power was P = 10 kW, and due to the mechanical and electrical efficiency (80%) and equation 12, R = 4 m. Considering Figs. 13 and 14, it can be seen that the part nearer to blade's roots has more chord length and chord length is reduced by moving away from the blade's roots. The same holds true for twist angle. It can be seen that blades designed for optimum power production have an increasingly large chord and twist angle as one gets closer to the blade root. Power coefficient curve for blade's length is presented in Fig. 15. Given Fig. 15, it can be seen that the largest share of power generation is relatively in the range of 30-90% blade length.

It should be noted that in the chart for Fig. 15 and given Eq. (27), if it becomes $r = R$, F = 0 and it will be C_P = 0 according to Eq. (33). But in the performed program it was never $r \neq R$ and thus the curve of Fig. 15 never interrupts the horizontal-axis because in the performed

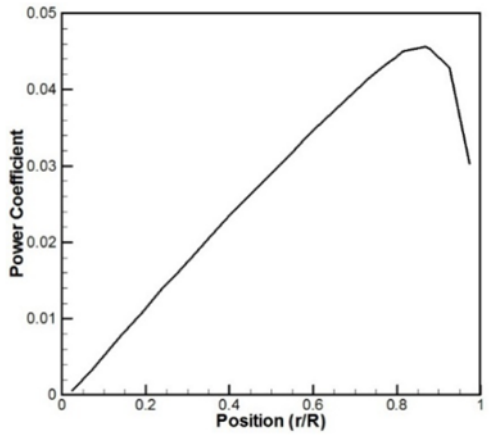

Fig. 15 Power coefficient in the blade's length

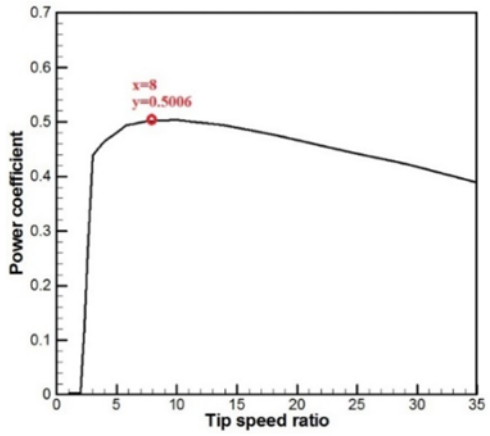

Fig. 17 C_P-λ based on the second view

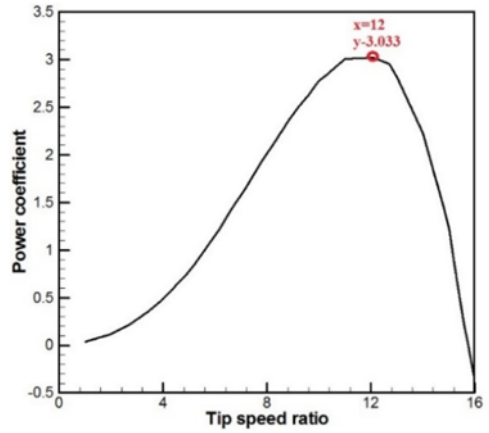

Fig. 16 C_P-λ based on the first view

program, "r" is the distance between centers of the divided "N" of the blade. Two different views exist for drawing C_P-λ diagram. The first view, attempts to depict C_P-λ diagram by fixing all the parameters in Eq. (33) except λ_i. The second view starts all calculations from the first step up to the last, from Eq. (12), by changing λ, and calculates C_P coefficient after the calculation of a' and a coefficients. In Figs. 16 and 17, C_P-λ is drawn for both of the two views.

As shown in Figs. 16 and 17, in the second view, the most amount of C_P is achieved equals to 0.5006 for $\lambda = 8$ while the most amount of C_P in the first view is almost six times of the second view and is occurred in $\lambda = 12$.

Weibull distribution was performed for the speed in 10 m, 30 m and 40 m heights in the considered stations. Furthermore, months of the year with the most wind speed and maximum power density were determined. Afterwards in Table 5, the result of blade design for this station is shown.

By selecting Kuriant18 turbine made by Kuriant Company and Vestas55 made by Vestas Company, and using performance curve and Weibull distribution for the Fadashk station, the amount of annually generated power by these selected wind turbines was obtained equal 10 kW (Table 5). Specifications of the selected wind turbines are shown in Fig. 18. Specifications of the chord length, twist angle and axial and angular contractions etc. for every 20 elements of the airfoil are shown in Table 6.

Table 5 Specifications of the designed blade

Item	Value
λ	8
Number of blades	3
Power required (kW)	10
Mechanical and electrical efficiency (%)	80
Rotor radius (m)	4
Optimal angle of attack (α)	6.60

4. Conclusions

In recent years, wind energy assessment has been conducted in many parts of the world. Accordingly, most of Iran regions have the significant potential for harnessing wind energy. In this study, hourly measured long term wind speed data of Fadashk region have been statistically analyzed. The most important outcomes of the study can be summarized as follows:

1. The Weibull distribution presented here indicates a good agreement with the data obtained from actual measurements.

2. March is the month that the mean wind speed is the highest all around the year ($\bar{U}$ = 9.7 m/s) and the lowest annual mean wind speed occurs in September ($\bar{U}$ = 2.81 m/s).

3. Annual average wind power density in this station was 285 W/m².

At the end, it worth mentioning that the current work is only a preliminary study in order to estimate the wind energy potential analysis of Fadashk region, in order to have a comprehensive wind data base and obtain good predictions prior to construction and installation of wind energy conversion systems. In assessing the wind power potential or choosing the suitable type of wind turbine, not only the wind data but also the site circumstances (terrain, different referred height, etc) should be considered that this issue can be addressed for application of new wind energy generation technology.[36]

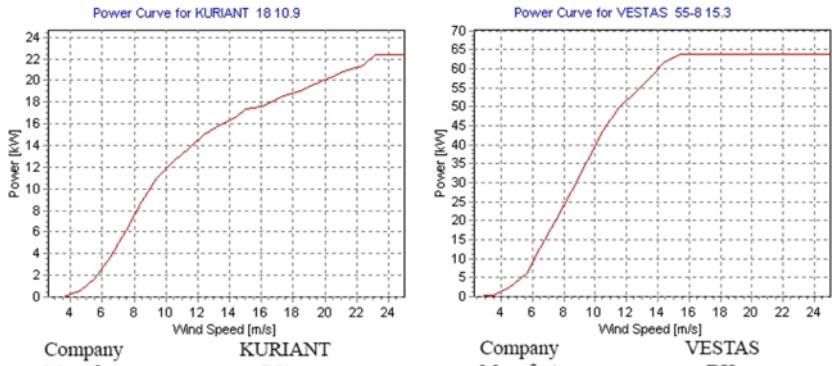

Company	KURIANT
Manufacturer	DK
Rated Power	18 kW
Small Generator	none
Variable Speed	no
Power control	Stall
Blade Type	KJ 5
Rotor Diameter	10,9 m
Swept Area	93 m2
Power per m2	0,193 kW/m2
Rpm at rated power	66,7 rpm
Rpm at cut in	0 rpm
Standard hub height(s)	15 m
Tower	Lattice

Company	VESTAS
Manufacturer	DK
Rated Power	55 kW
Small Generator	7.5 kW
Variable Speed	2 generator
Power control	Stall
Blade Type	ØKÆR
Rotor Diameter	15.3 m
Swept Area	184 m2
Power per m2	0.299 kW/m2
Rpm at rated power	50.4
Rpm at cut in	0 rpm
Standard hub height(s)	18 m
Tower	Lattice

Fig. 18 Specifications of the selected turbines

Table 6 Specifications of the 20 elements of the airfoil

r/R	Chord length c_i (m)	Relative velocity angle, φ_i (deg)	Angle of attack, α_i (deg)	Twist angle θ_T (deg)	Lift coefficient C_{l_i}	Axial contraction, a_i	Angular contraction, a_i'
0.05	1.319	52.460	8	23.85	0.912	0.274	1.787
0.10	1.25	39.357	8	22.048	0.912	0.303	0.415
0.15	1.198	30	8	20.240	0.912	0.316	0.183
0.20	1.137	23.69	8	18.43	0.912	0.323	0.101
0.25	1.077	19.36	8	16.62	0.912	0.326	0.0638
0.30	1.016	16.30	8	14.81	0.912	0.328	0.0436
0.35	0.955	14.02	8	13.01	0.912	0.329	0.0317
0.40	0.895	12.289	8	11.20	0.912	0.330	0.024
0.45	0.834	10.926	8	9.39	0.912	0.331	0.0188
0.50	0.773	9.82	8	7.58	0.912	0.331	0.01512
0.55	0.713	8.928	8	5.78	0.912	0.332	0.0124
0.60	0.652	8.176	8	3.972	0.912	0.332	0.01037
0.65	0.59	7.539	8	2.165	0.912	0.332	0.0088
0.70	0.53	6.990	7.995	0.357	0.9125	0.333	0.0075
0.75	0.47	6.512	7.990	-1.450	0.9123	0.334	0.00658
0.80	0.409	6.086	7.978	-3.25	0.9116	0.336	0.005796
0.85	0.349	5.65	7.905	-5.06	0.9077	0.344	0.005173
0.90	0.288	5.164	7.743	-6.870	0.8983	0.365	0.004712
0.95	0.227	4.476	7.345	-8.680	0.8689	0.419	0.00444
1	0.167	0.002	3.129	-10.487	0.4594	0.9999	0.0018202
	Linearization			Linearization			

REFERENCES

1. Nakata, T., Silva, D., and Rodionov, M., "Application of Energy System Models for Designing a Low-Carbon Society," Progress in Energy and Combustion Science, Vol. 37, No. 4, pp. 462-502, 2011.
2. Hosseini, S. E., Andwari, A. M., Wahid, M. A., and Bagheri, G., "A Review on Green Energy Potentials in Iran," Renewable and Sustainable Energy Reviews, Vol. 27, pp. 533-545, 2013.
3. Tzanakis, I., Hadfield, M., Thomas, B., Noya, S., Henshaw, I., and Austen, S., "Future Perspectives on Sustainable Tribology," Renewable and Sustainable Energy Reviews, Vol. 16, No. 6, pp. 4126-4140, 2012.

4. Chen, W. and Geng, W., "Fossil Energy Saving and CO_2 Emissions Reduction Performance, and Dynamic Change in Performance Considering Renewable Energy Input," Energy, Vol. 120, pp. 283-292, 2017.

5. Tsai, B.-H., Chang, C.-J., and Chang, C.-H., "Elucidating the Consumption and CO_2 Emissions of fossil Fuels and Low-Carbon Energy in the United States Using Lotka-Volterra Models," Energy, Vol. 100, pp. 416-424, 2016.

6. Schaeffer, R., Szklo, A. S., de Lucena, A. F. P., Borba, B. S. M. C., Nogueira, L. P. P., et al., "Energy Sector Vulnerability to Climate Change: A Review," Energy, Vol. 38, No. 1, pp. 1-12, 2012.

7. International Energy Agency, "World Energy Outlook 2014," https://www.iea.org/publications/freepublications/publication/WEO2014.pdf (Accessed 21 SEP 2017)

8. Lotfalipour, M. R., Falahi, M. A., and Ashena, M., "Economic Growth, CO_2 Emissions, and Fossil Fuels Consumption in Iran," Energy, Vol. 35, No. 12, pp. 5115-5120, 2010.

9. International Energy Agency, "World Energy Outlook 2010," https://www.worldenergyoutlook.org/media/weo2010.pdf (Accessed 21 SEP 2017)

10. Alamdari, P., Nematollahi, O., and Mirhosseini, M., "Assessment of Wind Energy in Iran: A Review," Renewable and Sustainable Energy Reviews, Vol. 16, No. 1, pp. 836-860, 2012.

11. Shezan, S. A., Julai, S., Kibria, M. A., Ullah, K. R., Saidur, R., et al., "Performance Analysis of an Off-Grid Wind-PV (Photovoltaic)-Diesel-Battery Hybrid Energy System Feasible for Remote Areas," Journal of Cleaner Production, Vol. 125, pp. 121-132, 2016.

12. Wesseh, P. K. and Lin, B., "A Real Options Valuation of Chinese Wind Energy Technologies for Power Generation: Do Benefits from the Feed-in Tariffs Outweigh Costs?" Journal of Cleaner Production, Vol. 112, Part 2, pp. 1591-1599, 2016.

13. He, Y., Xu, Y., Pang, Y., Tian, H., and Wu, R., "A Regulatory Policy to Promote Renewable Energy Consumption in China: Review and Future Evolutionary Path," Renewable Energy, Vol. 89, pp. 695-705, 2016.

14. Wüstenhagen, R., Wolsink, M., and Bürer, M. J., "Social Acceptance of Renewable Energy Innovation: An Introduction to the Concept," Energy Policy, Vol. 35, No. 5, pp. 2683-2691, 2007.

15. Kumar, I., Tyner, W. E., and Sinha, K. C., "Input-Output Life Cycle Environmental Assessment of Greenhouse Gas Emissions from Utility Scale Wind Energy in the United States," Energy Policy, Vol. 89, pp. 294-301, 2016.

16. Akpınar, A., "Evaluation of Wind Energy Potentiality at Coastal Locations Along the North Eastern Coasts of Turkey," Energy, Vol. 50, No. pp. 395-405, 2013.

17. Wiser, R., Bolinger, M., Heath, G., Keyser, D., Lantz, E., Macknick, J., Mai, T., and Millstein, D., "Long-Term Implications of Sustained Wind Power Growth in the United States: Potential Benefits and Secondary Impacts," Applied Energy, Vol. 179, pp. 146-158, 2016.

18. Purohit, I. and Purohit, P., "Wind Energy in India: Status and Future Prospects," Journal of Renewable and Sustainable Energy, Vol. 1, No. 4, Paper No. 042701, 2009.

19. Nedaei, M., Assareh, E., and Biglari, M., "An Extensive Evaluation of Wind Resource Using New Methods and Strategies for Development and Utilizing Wind Power in Mah-Shahr Station in Iran," Energy Conversion and Management, Vol. 81, pp. 475-503, 2014.

20. Jahangiri, M., Nematollahi, O., Sedaghat, A., and Saghafian, M., "Techno-Economical Assessment of Renewable Energies Integrated with Fuel Cell for Off Grid Electrification: A Case Study for Developing Countries," Journal of Renewable and Sustainable Energy, Vol. 7, No. 2, Paper No. 023123, 2015.

21. Tummala, A., Velamati, R. K., Sinha, D. K., Indraja, V., and Krishna, V. H., "A Review on Small Scale Wind Turbines," Renewable and Sustainable Energy Reviews, Vol. 56, pp. 1351-1371, 2016.

22. Saeidi, D., Mirhosseini, M., Sedaghat, A., and Mostafaeipour, A., "Feasibility Study of Wind Energy Potential in Two Provinces of Iran: North and South Khorasan," Renewable and Sustainable Energy Reviews, Vol. 15, No. 8, pp. 3558-3569, 2011.

23. Mostafaeipour, A., Sedaghat, A., Dehghan-Niri, A., and Kalantar, V., "Wind Energy Feasibility Study for City of Shahrbabak in Iran," Renewable and Sustainable Energy Reviews, Vol. 15, No. 6, pp. 2545-2556, 2011.

24. Fazelpour, F., Soltani, N., Soltani, S., and Rosen, M. A., "Assessment of Wind Energy Potential and Economics in the North-Western Iranian Cities of Tabriz and Ardabil," Renewable and Sustainable Energy Reviews, Vol. 45, pp. 87-99, 2015.

25. Keyhani, A., Ghasemi-Varnamkhasti, M., Khanali, M., and Abbaszadeh, R., "An Assessment of Wind Energy Potential as a Power Generation Source in the Capital of Iran, Tehran," Energy, Vol. 35, No. 1, pp. 188-201, 2010.

26. Dabbaghiyan, A., Fazelpour, F., Abnavi, M. D., and Rosen, M. A., "Evaluation of Wind Energy Potential in Province of Bushehr, Iran," Renewable and Sustainable Energy Reviews, Vol. 55, pp. 455-466, 2016.

27. Mostafaeipour, A., "Feasibility Study of Harnessing Wind Energy for Turbine Installation in Province of Yazd in Iran," Renewable and Sustainable Energy Reviews, Vol. 14, No. 1, pp. 93-111, 2010.

28. Mostafaeipour, A., Jadidi, M., Mohammadi, K., and Sedaghat, A., "An Analysis of Wind Energy Potential and Economic Evaluation in Zahedan, Iran," Renewable and Sustainable Energy Reviews, Vol. 30, pp. 641-650, 2014.

29. Mostafaeipour, A., Sedaghat, A., Ghalishooyan, M., Dinpashoh, Y., Mirhosseini, M., et al., "Evaluation of Wind Energy Potential as a Power Generation Source for Electricity Production in Binalood, Iran," Renewable Energy, Vol. 52, pp. 222-229, 2013.

30. Jahangiri, M., Ghaderi, R., Haghani, A., and Nematollahi, O., "Finding the Best Locations for Establishment of Solar-Wind Power Stations in Middle-East Using GIS: A Review," Renewable and Sustainable Energy Reviews, Vol. 66, pp. 38-52, 2016.

31. Bai, C.-J., Chen, P.-W., and Wang, W.-C., "Aerodynamic Design and Analysis of a 10 kW Horizontal-Axis Wind Turbine for Tainan, Taiwan," Clean Technologies and Environmental Policy, Vol. 18, No. 4, pp. 1151-1166, 2016.

32. Manwell, J. F., McGowan, J. G., and Rogers, A. L., "Wind Energy Explained: Theory, Design and Application," John Wiley & Sons, 2nd Ed., 2009.

33. Burton, T., Jenkins, N., Sharpe, D., and Bossanyi, E., "Wind Energy Handbook," John Wiley & Sons, 2001.

34. Yurdusev, M. A., Ata, R., and Çetin, N. S., "Assessment of Optimum Tip Speed Ratio in Wind Turbines Using Artificial Neural Networks," Energy, Vol. 31, No. 12, pp. 2153-2161, 2006.

35. Maldonado, V., Castillo, L., Thormann, A., and Meneveau, C., "The Role of Free Stream Turbulence with Large Integral Scale on the Aerodynamic Performance of an Experimental Low Reynolds Number S809 Wind Turbine Blade," Journal of Wind Engineering and Industrial Aerodynamics, Vol. 142, pp. 246-257, 2015.

36. Canale, M., Fagiano, L., and Milanese, M., "Kitegen: A Revolution in Wind Energy Generation," Energy, Vol. 34, No. 3, pp. 355-361, 2009.